PPPL-2504

UC-426

PPPL-2504

SPECTRA IN THE 60 Å - 345 Å WAVELENGTH REGION OF ELEMENTS INJECTED INTO THE PLT TOKAMAK

By

A. Wouters, J.L. Schwob, S. Suckewer,
J.F. Seely, U. Feldman, J.H. Dave

MARCH 1988

PLASMA
PHYSICS
LABORATORY

PRINCETON UNIVERSITY
PRINCETON, NEW JERSEY

PREPARED FOR THE U.S. DEPARTMENT OF ENERGY,
UNDER CONTRACT DE-AC02-76-CHO-3073.

NOTICE

Printed in the United States of America

Available from:

National Technical Information Service
U.S. Department of Commerce
5285 Port Royal Road
Springfield, Virginia 22161

Price Printed Copy $ * ; Microfiche $4.50

*Pages	NTIS Selling Price	
1-25	$7.00	For documents over 600 pages, add $1.50 for each additional 25-page increment.
25-50	$8.50	
51-75	$10.00	
76-100	$11.50	
101-125	$13.00	
126-150	$14.50	
151-175	$16.00	
176-200	$17.50	
201-225	$19.00	
226-250	$20.50	
251-275	$22.00	
276-300	$23.50	
301-325	$25.00	
326-350	$26.50	
351-375	$28.00	
376-400	$29.50	
401-425	$31.00	
426-450	$32.50	
451-475	$34.00	
476-500	$35.50	
500-525	$37.00	
526-550	$38.50	
551-575	$40.00	
567-600	$41.50	

PPPL--2504

DE88 009340

Spectra in the 60 Å - 345 Å Wavelength Region of Elements Injected into the PLT Tokamak

A. Wouters, J.L. Schwob*, and S. Suckewer
Princeton Plasma Physics Laboratory
Princeton University
Princeton, NJ 08544

J.F. Seely and U. Feldman
E.O. Hulbert Center for Space Research
Naval Research Laboratory
Washington, DC 20375-5000

J.H. Davé
Applied Research Corporation
8201 Corporate Drive
Landover, MD 20785

* Racah Institute, Hebrew University of Jerusalem

ABSTRACT

High resolution spectra of the elements Fe, Ni, Zn, Ge, Se, and Mo injected into the PLT tokamak were recorded by the 2-meter Schwob-Fraenkel soft X-ray multichannel spectrometer (SOXMOS). Spectra were recorded every 50 ms during the time before and after injection. The spectral lines of the injected element were very strong in the spectrum recorded immediately after injection, and the transition in the injected element were easily distinguished from the transitions in the intrinsic elements (C, O, Ti, Cr, Fe, and Ni). An accurate wavelength scale was established using well-known reference transitions in the intrinsic elements. The spectra recorded just prior to injection were subtracted from the spectra recorded after injection, and the resulting spectrum was composed almost entirely of transitions from the injected element. A large number of $\Delta n = 0$ transitions between the ground and the first excited configurations in the Li I through K I isoelectronic sequences of the injected elements were identified in the wavelength region 60 Å to 345 Å.

Introduction

The PLT tokamak represents a very useful tool for the study of the spectra of highly charged ions. Electron temperatures up to 2.5 keV occur in the center of the ohmically heated discharge and persist for a time period up to 1 sec. Since this time period is typically long compared to the ionization and recombination times of the highly charged ions from the wall material, the spectra of these ions are essentially steady during most the plateau regime of the discharge. The spectra of transiently injected elements are easily detected against the steady background spectra of the intrinsic elements.

Time-resolved spectra of the intrinsic elements (C, O, Ti, Cr, Fe, and Ni) and of injected elements were recorded using the 2-meter Schwob-Fraenkel soft X-ray multichannel spectrometer (SOXMOS). Spectra were taken every 50 ms in the 60 Å - 345 Å wavelength region. Corrections were made for nonlinearities in the multichannel detector and the fiber optic transmission line, and an accurate wavelength scale was established using well-known reference lines. The spectra from the intrinsic elements were presented in Ref. 1. In the present paper, we present the spectra of the injected elements Fe, Ni, Zn, Ge, Se, and Mo.

Experimental Configuration

The spectra of the injected elements were recorded by the SOXMOS spectrometer[2-4] fitted with a 600 lines/mm grating with a blaze angle of 3° 31'. The spectra were detected by a flat MgF_2-coated microchannel plate (MCP) that was coupled to a 1024-pixel photodiode array by a fiber optic transmission line. For each discharge, data in a wavelength interval approximately 50 Å wide could be recorded, and the wavelength region from 60 Å to 345 Å was covered by moving the MCP. Spectral scans were recorded every 50 ms throughout the discharge, and typically more than 10 usable scans with strong

spectral features were obtained on each discharge.

The elements were injected during the plateau regime of ohmically heated discharges using the laser blowoff technique. Before the time of injection, the recorded spectra were composed of transitions in highly charged ions of the elements from the wall material (C, O, Ti, Cr, Fe, and Ni). We shall refer to the spectrum of the intrinsic elements as the background spectrum.

Shown in Fig. 1 are the spectra in the wavelength region 155 Å to 215 Å recorded just before and after Mo injection. The spectrum shown in Fig. 1 (a) was recorded just before injection and is composed of transitions from the intrinsic elements. In the spectrum recorded 50 ms later, Fig. 1 (b), transitions from highly charged Mo ions appear superimposed on the background spectrum. The Mo transitions are diminished in the next spectrum recorded 50 ms later, Fig.1 (c).

The spectra shown in Fig. 1 are typical of the spectra of the injected elements. In general, the intensity of the background continuum and line intensities increases slightly during injection, probably due to increased electron density, but the background spectrum is otherwise not significantly perturbed. The transitions from the injected element appear strong in the spectral scans recorded immediately after injection and diminish during the following several scans. Since the relative intensities of the background spectral features do not vary significantly during injection, it is possible to difference the scans recorded before and after injection and thereby suppress the background spectrum. This is illustrated in Figs. 2-5 for the case of Mo injection. For example, the spectrum shown in Fig. 4 was obtained by substracting the spectrum of Fig. 1 (a) from the spectrum of Fig. 1 (b). The difference spectrum is composed almost entirely of transitions from the injected element. In some cases, the relative intensities of some background transitions may vary slightly during injection, but this variation is always small. This is illustrated in Fig. 4, where the O VI transition at 173.0 Å decreases during injection and appears below the continuum level in the difference spectrum.

Measured Wavelengths

The wavelength scale was established using transitions from the intrinsic elements recorded before injection. The basic technique for establishing the wavelength scale was described in Ref. 1. In the present work, several improvements in this technique have been made.

The wavelength of a spectral feature is given by the grating equation

$$\lambda = d\ (\cos\ \alpha - \cos\ \beta) \quad , \tag{1}$$

where d^{-1} is the number of lines per unit length of grating, α is the angle of incidence, and β is the angle of diffraction. As derived in Ref. 1, the effective angular position β of a pixel p on the MCP, measured from the angular position β_o of the tangential pixel p_o, is

$$\beta = \beta_o + \cot^{-1}\ [(2RN/M)/(p-p_o) + \cot\ \beta_o] \text{ for } p \neq p_o \ , \tag{2}$$

where R is the radius of the Rowland circle, M is the magnification of the fiber optic transmission line, and N is the number of pixels per unit length on the detector. The angle β_o of the tangential pixel changes when the MCP is moved along the Rowland circle to cover different wavelength regions. The tangential pixel is ideally fixed at the midpoint of the MCP at pixel number 512, and the

quantity RN/M is also fixed. Using the known wavelengths and expected pixel positions of the reference transitions in the background spectrum, it is possible to correct for nonlinearities in the fiber optic and the pixel array. The correction curve is ideally characteristic of the MCP and detector and is independent of the MCP position on the Rowland circle. This was the approach used in Ref. 1. In the present work, it was found that the correction curves derived from spectra at different MCP positions varied slightly. After taking into account the uncertainties in the measured positions of the reference transitions, the variation in the correction curve was greater than expected and was attributed to slight changes in the geometry of the spectrometer. For example, the tangential pixel, which is nominally the midpoint of the detector at pixel number 512, may change owing to slight imperfections in the MCP carriage and guide. The effective radius of the Rowland circle R may also slightly change for the same reason. In the present work, the best values for the quantities RN/M, p_o, and β_o in Eq. (2) were determined for each plasma discharge by a least-squares fit to the reference transitions.

The wavelength scale was determined as follows. The pixel positions of the spectral features in the background spectra recorded before injection were determined. A computer program determined the centroid of each spectral feature, and the wavelengths of the spectral features were calculated using initial values for RN/M, p_o, and β_o. These initial wavelengths were typically accurate to approximately ± 0.1 Å. The calculated wavelengths were matched to a list of reference wavelengths. The list of reference transitions was essentially the same as listed in Ref. 1 with a few improvements. Typically 20 to 30 reference lines could be initially identified, and the quantities RN/M , p_o, and β_o were varied to minimize the differences between the calculated and reference wavelengths. On each interation, additional spectral features were identified, and the process continued until all of the

features in the background spectrum were identified. The total number of background features identified depended on the density of spectral features in a given wavelength region and was typically 40 to 60. Using the final values of RN/M, p_o, and β_o, the differences between the calculated and reference wavelengths of strong and unblended features were less than ± 0.02 Å. The wavelength discrepancies for a few reference features were consistently larger than ± 0.05 Å, and these reference wavelengths were removed from the list. It was found that the pixel positions of reference features recorded near the large-pixel-number end of the MCP consistently deviated from the expected pixel positions by up to 8 pixels. This was also found in the earlier work (see Fig. 2 of Ref. 1) and is attributable to a relatively large nonlinearity in this MCP, or fiber optic, near the large-pixel-number end. As only correction for this discrepancy, an ab initio pixel correction 0.04 (p-800) was added to the initial pixel position p for all pixels above 800. The final absolute wavelength scale is believed to be accurate to ± 0.01 Å across the entire MCP.

The wavelengths of the spectral features in the injected spectra were calculated using the final values of RN/M, p_o, and β_o determined from the background spectra on each discharge. The background spectrum was substracted as discussed above. A computer program measured the centroids of the spectral features, and the wavelengths were calculated using Eqs. (1) and (2). The line widths of the spectral features were 0.1 Å to 0.3 Å and the maximum uncertainty in the determined wavelengths was ± 0.02 Å for intense and unblended features.

Line Identifications

The identification of the spectral features in the injected spectra was based on previous observations[5-26] or on the recommended wavelengths of Edlen.[27-31] The identifications and wavelengths are

presented in Table 1. Transitions in the isoelectronic sequences Li I through K I have been identified. With the exception of several Na I transitions, all of these transitions are of the type $\Delta n = 0$ and terminate on levels within the ground configurations of the ions.

Nearly all of the transitions in Fe, Ni, and Zn were identified. A number of transitions in Ge, Se, and Mo remain to be identified. These unidentified transitions generally fall at short wavelengths (see Fig. 2 for Mo) and are probably transitions in the Si I through K I isoelectronic sequences. The unambiguous identification of these transitions depends on the comparison of observed and calculated wavelengths along the isoelectronic sequence, and this will be the subject of future papers. This future work will also include more recently recorded data for selected elements up to ytterbium (Z=70). Such a comparison of observed wavelengths and wavelengths calculated using the Grant[32] program has been done for three Ar-like transitions and for the Mg-like $3s^2\ {}^1S_0$ - $3s3p\ {}^3P_1$ transition[33], and these identifications are included in Table 1.

Conclusions

Numerical techniques were developed to analyze the spectra from the SOXMOS spectrometer. An accurate wavelength scale was established using reference transitions in the spectrum of the intrinsic elements recorded before injection. The wavelength of transitions from the injected elements Fe, Ni, Zn, Ge, Se, and Mo were measured, and a large number of $\Delta n = 0$ transitions were identified. The accurately measured wavelengths will permit the identification of additional transitions in the Si I through K I isoelectronic sequences of the elements Ge, Se, and Mo. The numerical techniques and isoelectronic analyses will also be applied to the spectra of selected elements up to Z=70 that have been recently recorded.

References

1. J. Dave, U. Feldman, J.F. Seely, A. Wouters, S. Suckewer, E. Hinnov, and J.L. Schwob, "Time-resolved spectra in the 80-340 Å wavelength region from PLT tokamak plasmas," J. Opt. Soc. Am. B 4, 635 (1987).
2. A.S. Filler, J.L. Schwob, and B.S. Fraenkel, in Proceedings of the 5th International Conference on UV Radiation Physics, Castex, M. Pouey and N. Pouey, eds. (Centre National de la Recherche Scientifique, Paris, 1977), Vol. 1, p. 86.
3. J.L. Schwob, A.W. Wouters, S. Suckewer, and M. Finkenthal, "High-resolution duo-multichannel soft X-ray spectrometer for tokamak plasma diagnostics," Rev. Sci. Instrum. 58, 1601 (1987).
4. J.L. Schwob, A. Wouters, S. Suckewer, F.P. Boody, and M. Finkenthal, "Time-resolved spectra in the 5-300 Å region emitted from the PLT and TFTR tokamak plasmas," Proc. 8th Int. Coll. on EUV and X-ray Spectroscopy of Astrophysical and Laboratory Plasmas, IAU Coll. No. 86 (1984).
5. S. Goldsmith and B.S. Fraenkel, "Classification of new multiplets in the extreme-ultraviolet spectra of nickel, copper, and zinc," Astrophys. J. 161, 317 (1970).
6. W.E. Behring, L. Cohen, and U. Feldman, "The solar spectrum: wavelengths and identifications from 60 to 385 angstroms," Astrophys. J. 175, 493 (1972).
7. B.C. Fawcett and R.W. Hayes, "The classification of Ni XI to XVII and Co X to XVII emission lines from $3s^2 3p^n$ - $3s3p^{n+1}$ and $3p^n$ - $3p^{n-1}3d$ transitions and the identifications of nickel solar lines," J. Phys. B 5, 366 (1972).
8. B.C. Fawcett, R.D. Cowan, and R.W. Hayes, "New classifications of highly ionized Ni, Co, Cr, V, and isoelectronic spectra," J. Phys. B 5, 2143 (1972).

9. L.A. Svensson, J.O. Ekberg, and B. Edlen, "The identification of Fe IX and Ni XI in the solar corona," Solar Phys. 34, 173 (1974).

10. B.C. Fawcett and R.W. Hayes, "Spectra in the period between copper and bromine produced with the aid of a 4 GW laser," J. Opt. Soc. Am. 65, 623 (1975).

11. W.E. Behring, L. Cohen, U. Feldman, and G.A. Doschek, "The solar spectrum: wavlengths and identifications from 160 to 770 angstroms," Astrophys. J. 203, 521 (1976).

12. P.G. Burkhalter, J. Reader, and R.D. Cowan, "Spectra of Mo XXX, XXXI and XXXII from a laser-produced plasma," J. Opt. Soc. Am. 67, 1521 (1977).

13. G.E. Bromage, R.D. Cowan, and B.C. Fawcett, "Atomic structure calculations involving optimization of radial integrals: energy levels and oscillator strengths for Fe XII and Fe XIII 3p-3d and 3s-3p transitions," Mon. Not. R. Astr. Soc. 183, 19 (1978).

14. E. Ya. Kononov, A.N. Ryabtsev, and S.S. Churilov, "Spectra of sodium-like ions Cu XIX - Br XXV," Phys. Scripta 19, 328 (1979).

15. B.C. Fawcett and A.T. Hatter, "Spectra of the $3s^2 3p^n$ - $3s3p^{n+1}$ transition arrays emitted from nickel and cobalt ions," Astron. Astrophys. 84, 78 (1980).

16. M. Finkenthal, E. Hinnov, S. Cohen, and S. Suckewer, "The $3s^2\ {}^1S_0$ - $3s3p\ {}^3P_1$ magnesium sequence intercombination lines from Sc X to Mo XXXI observed in the PLT tokamak," Phys. Lett. 91, 284 (1982).

17. B.C. Stratton, W.L. Hodge, H.W. Moos, J.L. Schwob, S.Suckewer M. Finkenthal, and S. Cohen, "Spectra of germanium and selenium in the 50-350 Å region from the PLT tokamak plasma," J. Opt. Soc. Am. 73, 877 (1983).

18. J. Reader, "$3s^2$ - 3s3p and 3s3p - 3s3d transitions in magnesiumlike ions from Sr^{26+} to Rh^{33+}," J. Opt. Soc. Am. 73, 796 (1983).

19. N.J. Peakcock, M.F. Stamp, and J.D. Silver, "Highly-ionized atoms in fusion research plasmas," Phys. Scripta T8, 10 (1984).
20. W.E. Behring, J.F. Seely, S. Goldsmith, L Cohen, M.Richardson and U. Feldman, "Transitions of the type 2s-2p in highly ionized Cu, Zn, Ga, and Ge," J. Opt. Soc. Am. B 2, 886 (1985).
21. K.D. Lawson, and N.J. Peacock, "The analysis of the n = 2 - 2 transitions in the XUV spectra of Cr to Ni," J. Phys. B 13, 3313 (1980).
22. E. Hinnov, F. Boody, S. Cohen, U. Feldman, J. Hosea, K. Sato, J.L. Schwob, S. Suckewer, and A. Wouters, "Spectrum lines of highly ionized zinc, germanium, selenium, zirconium, molybdenum, and silver injected into Princeton Large Torus and Tokamak Fusion Test Reactor tokamak discharges," J. Opt. Soc. Am. 3, 1288 (1986).
23. J. Sugar and V. Kaufman, "Wavelengths and energy levels of Zn XII to Zn XX," Phys. Scripta 34, 797 (1986).
24. M. Finkenthal, B.C. Stratton, H.W. Moos, W.L. Hodge, S. Suckewer, S. Cohen, P. Mandelbaum, and M. Klapisch, "Spectra of highly ionized zirconium and molybdenum in the 60 - 150 Å range from PLT tokamak plasmas," J. Phys. B 18, 4393 (1985).
25. J. Reader, V. Kaufman, J. Sugar, J.O. Ekberg, U. Feldman, C.M. Brown, J.F. Seely, and W.L. Rowan, "3s - 3p, 3p - 3d, and 4d - 4f transitions of sodiumlike ions," J. Opt. Soc. Am. B 4, 1821 (1987).
26. U. Feldman, L. Katz, W. Behring, and L. Cohen, "Spectra of Fe, Co, Ni, and Cu isoelectronic with Na I and Mg I," J. Opt. Soc. Am. 61, 91 (1971).
27. B. Edlen, "Comparison of theoretical and experimental level values of the n = 2 complex in ions isoelectronic with Li, Be, O, and F," Phys. Scripta 28, 51 (1983).
28. B. Edlen, "Comparison of theoretical and experimental level values of the n = 2 configurations in the boron isoelectronic sequence," Phys. Scripta 28, 483 (1983).

29. B. Edlen, "Comparison of theoretical and experimental level values of the n = 2 configurations in the nitrogen isoelectronic sequence," Phys. Scripta 30, 135 (1984).
30. B. Edlen, "Comparison of theoretical and experimental level values of the n = 2 configurations in the carbon isoelectronic sequence," Phys. Scripta 31, 345 (1985).
31. B. Edlen, "Na-like spectra of the elements calcium through copper, X IX - Cu XIX," Z Physik 100, 621 (1936).
32. I.P. Grant, B.J. McKenzie, and P.H. Norrington, "An atmoic multiconfiguration Dirac-Fock package," Computer Phys. Commun. 21, 207 (1980).
33. J.F. Seely, J.O. Ekberg, U. Feldman, J.L. Schwob, S. Suckewer, and A. Wouters, "Wavelengths for the $3s^2\ {}^1S_0$ - $3s3p\ {}^3P_1$ transition of the magnesiumlike ions Fe^{14+} - Nd^{48+}," J. Opt. Soc. Am. B 5 (in press).

Table I. Classification of Spectral Lines, Presently Measured Wavelengths, and Previous Wavelengths.

Transition	Wavelengths (in Angstroms)											
	Pres	Prev	Pres	Prev	Pres	Prev	Pres	Prev	Pres	Prev	Pres	Prev
Li I												
	Fe XXIV		Ni XXVI		Zn XXVIII		Ge XXX		Se XXXII		Mo XL	
2s-2p												
$^2S_{1/2}$-$^2P_{3/2}$	192.04	192.01[a]	165.39	165.38[a]	142.40	142.44[a]	122.76[B]	122.66[a]		105.64[a]		
$^2S_{1/2}$-$^2P_{1/2}$	255.16	255.08[a]	234.10	234.09[a]		215.99[a]		200.18[a]		186.25[a]		
Be I												
	Fe XXIII		Ni XXV		Zn XXVII		Ge XXIX		Se XXXI		Mo XXXIX	
$2s^2$-2s2p												
$^1S_0$-$^1P_1$	132.90	132.88[a]	117.98[B]	117.94[a]	104.57[B]	104.67[a]	92.78	92.81[a]		82.18[a]		
$^1S_0$-$^3P_1$	263.71	263.74[a]	238.89	238.86[a]	217.66	217.66[a]		199.46[a]		183.75[a]		

B I

	Fe XXII		Ni XXIV		Zn XXVI		Ge XXVIII		Se XXX		Mo XXXVIII
$2s^2 2p - 2s 2p^2$											
$^2P_{1/2}-^2P_{3/2}$	100.75	100.77[b]		87.46[b]		75.82[b]		65.64[b]		56.74[b]	
$^2P_{1/2}-^2P_{1/2}$	102.22[B]	102.22[b]		88.61[b]		76.8[b]		66.4[b]		57.3[b]	
$^2P_{3/2}-^2P_{3/2}$	114.39	114.41[b]	102.10[B]	102.10[b]		91.17[b]		81.37[b]		72.55[b]	
$^2P_{3/2}-^2P_{1/2}$	116.25	116.27[b]	103.68[S]	103.68[b]		92.6[b]		82.6[b]		73.5[b]	
$^2P_{1/2}-^2S_{1/2}$	117.19	117.18[b]	104.61	104.63[b]	93.62	93.5[b]		83.5[b]		74.6[b]	
$^2P_{1/2}-^2D_{3/2}$	135.80	135.76[b]	118.55	118.47[b]	103.70	103.60[b]	90.64	90.73[b]		79.56[b]	
$^2P_{3/2}-^2D_{5/2}$	156.00	155.94[b]	138.78	138.73[b]		123.20[b]		109.04[b]		96.12[b]	

C I

	Fe XXI		Ni XXIII		Zn XXV		Ge XXVII		Se XXIX	Mo XXXVII
$2s^22p^2-2s2p^3$										
$^3P_0-^3S_1$		91.27[c]	79.96	79.97[c]		70.02[c]	61.16	61.21[c]	53.41[c]	
$^3P_1-^3S_1$	97.91	97.86[c]	87.64	87.67[c]	78.71	78.71[d]	70.67	70.74[c]	63.55[c]	
$^1D_2-^1P_1$	98.32[B]	98.36[c]	87.98[S]	87.99[c]		78.89[c]		70.79[c]	63.52[c]	
$^3P_2-^1D_2$	99.06	99.03[c]		87.53[c]	77.13	77.11[d]		67.66[c]	59.05[c]	
$^3P_2-^3S_1$	102.22[B]	102.21[c]	91.87	91.87[c]	82.62	82.64[d]	74.39	74.30[d]	66.72[c]	
$^3P_0-^3P_1$		108.11[c]	92.71	92.72[c]	79.39	79.46[c]	67.97	68.07[c]	58.32[c]	
$^1D_2-^1D_2$	113.34[B]	113.29[c]	102.10[B]	102.07[c]		92.15[c]	83.21	83.14[c]	74.80[c]	
$^3P_1-^3P_0$	118.65[B]	118.69[c]		104.70[c]		92.52[c]		81.84[c]	72.42[c]	
$^3P_2-^3P_2$	121.19	121.19[c]	106.04[B]	106.05[c]	92.79	92.85[d]		81.37[d]	71.56[c]	
$^3P_2-^3P_1$	123.85	123.82[c]		109.09[c]		96.11[c]		84.66[c]	74.57[c]	
$^3P_0-^3D_1$	128.64	128.73[c]	111.84	111.83[c]	97.43	97.45[d]	85.12	85.08[c]	74.49[c]	
$^3P_1-^3D_2$	142.13	142.14[c]	126.62	126.59[c]	113.01	112.98[c]	100.72	100.82[c]	89.77[c]	
$^3P_2-^3D_3$	145.68	145.70[c]	128.36	128.32[c]		112.93[c]		99.28[c]	87.19[c]	
$^1D_2-^3D_3$	178.92	178.85[c]	162.18	162.19[c]		148.32[c]		136.60[c]	126.54[c]	

N I

	Fe XX		Ni XXII		Zn XXIV		Ge XXVI	Se XXVIII	Mo XXXVI
$2s^2 2p^3 - 2s 2p^4$									
$^2D_{3/2} - ^2P_{1/2}$	83.23	83.23[e]		72.52[e]	63.28	63.33[e]	55.38[e]	48.46[e]	
$^2D_{3/2} - ^2P_{3/2}$	90.54	90.59[e]		80.56[e]	71.87	71.92[d]	64.34[e]	57.68[e]	
$^2D_{5/2} - ^2P_{3/2}$		93.78[e]	84.09	84.07[e]	75.52	75.50[d]	67.84[d]	60.90[e]	
$^2D_{3/2} - ^2S_{1/2}$	94.59	94.64[e]		84.25[e]	75.33[B]	75.29[d]	67.43[d]	60.40[e]	
$^4S_{3/2} - ^2D_{3/2}$	95.95	95.92[e]		85.03[e]	75.33[B]	75.31[e]	66.51[e]	58.50[e]	
$^2P_{3/2} - ^2P_{1/2}$	98.32[B]	98.35[e]	88.02	88.01[e]		78.96[d]	70.99[d]	63.83[e]	
$^2D_{3/2} - ^2D_{3/2}$	110.59	110.63[e]	98.17	98.18[e]	87.67	87.69[d]	78.70[d]	70.87[e]	
$^2D_{5/2} - ^2D_{5/2}$	113.34[B]	113.35[e]	100.60	100.61[e]	89.52	89.47[d]	79.64[d]	70.84[e]	
$^4S_{3/2} - ^4P_{1/2}$	118.65[B]	118.68[e]	103.33	103.31[e]	90.06	90.05[d]	78.56[e]	68.70[e]	
$^4S_{3/2} - ^4P_{3/2}$	121.87	121.84[e]	106.04[B]	106.05[e]	92.23	92.18[d]	80.08[d]	69.51[e]	
$^4S_{3/2} - ^4P_{5/2}$	132.90[B]	132.84[e]	117.98[B]	117.92[e]	104.57[B]	104.54[d]	92.47[e]	81.60[e]	

O I

	Fe XIX		Ni XXI		Zn XXIII		Ge XXV		Se XXVII		Mo XXXV
$2s^22p^4$-$2s2p^5$											
$^1D_2$-$^1P_1$	91.01	91.01[a]	81.71	81.70[a]		73.59[a]		66.38[a]		59.88[a]	39.16[a]
$^3P_2$-$^3P_1$	101.56	101.56[a]	88.85	88.82[a]	77.93	77.95[a]		68.61[a]		60.58[a]	37.73[a]
$^1S_0$-$^1P_1$	106.12	106.11[a]		97.15[a]		89.79[a]		83.63[a]		78.33[a]	62.29[a]
$^3P_1$-$^3P_0$		106.32[a]	93.91	93.93[a]	83.15	83.22[a]		73.88[a]		65.67[a]	41.17[a]
$^3P_2$-$^3P_2$	108.34	108.36[a]	95.87[8]	95.86[a]	85.02	85.02[a]		75.51[a]		67.12[a]	41.99[a]
$^3P_0$-$^3P_1$	109.93	109.95[a]	96.82	96.80[a]		85.29[a]		75.21[a]		66.41[a]	41.04[a]
$^3P_1$-$^3P_1$	111.76	111.70[a]	100.27	100.24[a]	90.55	90.58[a]		82.38[a]		75.39[a]	55.93[a]
$^3P_1$-$^3P_2$	120.03	119.99[a]	109.26	109.31[a]	100.27	100.28[a]	92.44	92.53[a]		85.81[a]	65.83[a]

F I

	Fe XVIII		Ni XX		Zn XXII		Ge XXIV		Se XXVI		Mo XXXIV
$2s^22p^5$-$2s2p^6$											
$^2P_{3/2}$-$^2S_{1/2}$	93.89	93.93[a]	83.20	83.18[a]	73.91	73.94[a]		65.90[a]	58.85[5]	58.84[a]	37.66[a]
$^2P_{1/2}$-$^2S_{1/2}$	103.91	103.94[a]	94.51	94.50[a]	86.55	86.54[a]		79.75[a]		73.87[a]	56.54[a]

Na I

	Fe XVI		Ni XVIII		Zn XX		Ge XXII		Se XXIV		Mo XXXII	
3s-3p												
$^2S_{1/2}$-$^2P_{3/2}$	335.41	335.40[f]	292.00	291.99[g]	256.40	256.37[g]	226.53	226.50[g]	201.01	201.02[g]	127.86	127.87[g]
$^2S_{1/2}$-$^2P_{1/2}$		360.76[f]	320.55	320.57[g]	288.14	288.18[g]	261.47	261.50[g]	239.13	239.12[g]	176.64	176.65[g]
3p-3d												
$^2P_{1/2}$-$^2D_{3/2}$	251.09	251.07[f]	220.43	220.42[g]	195.43	195.38[g]	174.50[B]	174.39[g]	156.43	156.45[g]	104.29[B]	104.29[g]
$^2P_{3/2}$-$^2D_{5/2}$	262.98	262.98[f]	233.78	233.76[g]	210.18	210.16[g]	190.65	190.61[g]	174.10	174.10[g]	126.99	126.98[g]
$^2P_{3/2}$-$^2D_{3/2}$		265.00[g]		236.33[g]	213.20	213.33[g]	194.47	194.43[g]	178.61	178.61[g]	134.64	134.62[g]
3d-4f												
$^2D_{5/2}$-$^2F_{7/2}$	66.36	66.36[g]	52.73[S]	52.72[g]	42.91[S]	42.92[g]	35.61[S]	35.64[g]		30.08[g]		17.15[g]
3s-4p												
$^2S_{1/2}$-$^2P_{3/2}$	50.36	50.35[z]	41.03[S]	41.02[t]	33.97[S]	34.04[h]		28.71[h]				
3p-4d												
$^2P_{3/2}$-$^2D_{5/2}$	54.76	54.73[z]		44.35[z]	36.72[S]	36.71[h]	30.87[S]	30.89[h]				
3p-4s												
$^2P_{3/2}$-$^2S_{1/2}$	63.70	63.72[z]		51.04[t]		41.82[h]		34.92[h]				
4d-5f												
$^2D_{5/2}$-$^2F_{7/2}$	144.21	144.25[i]		114.74[i]								
4f-5g												
$^2F_{7/2}$-$^2G_{9/2}$	156.90	156.88[i]	124.02	124.04[i]								

Mg I

	Fe XV		Ni XVII		Zn XIX		Ge XXI		Se XXIII		Mo XXXI	
$3s^2$-3s3p												
$^1S_0$-$^1P_1$	284.15	284.16[f]	249.21	249.18[f]	220.59	220.58[m]	196.55	196.57[k]	176.05	175.92[k]	116.02	115.99[l]
$^1S_0$-$^3P_1$		417.26[f]		366.82[u]	326.44		293.20[B]	293.4[x]	265.84	265.7[x]	190.43	190.5[x]
3s3p-3s3d												
$^3P_0$-$^3D_1$	224.79	224.75[r]	197.39	197.39[v]		175.02[k]						
$^3P_1$-$^3D_2$	227.22	227.21[f]	199.84	199.87[v]		177.66[m]		159.14[k]			96.58	96.56[j]
$^3P_2$-$^3D_3$	233.79	233.86[f]	207.43	207.50[v]	186.31	186.35[m]	168.92	168.90[k]	154.14	154.04[k]	112.77	112.65[l]
$^1P_1$-$^1D_2$	243.79	243.79[f]	215.90[B]	215.89[v]	193.33	193.39[m]	174.50[B]	174.78[k]	158.93	158.86[k]	113.99	113.90[l]

Al I

	Fe XIV		Ni XVI		Zn XVIII		Ge XX		Se XXII		Mo XXX	
$3s^23p-3s^23d$												
$^2P_{1/2}-^2D_{3/2}$	211.33	211.32[f]	185.20	185.22[f]	164.06[B]	164.15[m]	146.51[B]	146.52[o]	131.61	131.66[o]	86.86	86.86[o]
$^2P_{3/2}-^2D_{5/2}$	219.13	219.12[f]	194.01	194.04[n]	173.94	173.99[m]	157.49	157.55[o]	143.61	143.65[o]	104.29[B]	104.33[o]
$^2P_{3/2}-^2D_{3/2}$	220.06	220.08[f]	195.26	195.27[n]	175.57	175.52[m]	159.31	159.25[o]	145.76	145.80[o]	105.65	105.59[o]
$3s^23p-3s3p^2$												
$^2P_{1/2}-^2P_{3/2}$		252.20[f]	218.44	218.39[n]	190.67	190.71[m]	167.57	167.49[o]	147.67	147.63[o]	92.53	92.55[o]
$^2P_{1/2}-^2P_{1/2}$	257.38	257.39[f]	223.08	223.09[n]	194.68	194.80[m]	170.75	170.81[o]	150.32[B]	150.34[o]	91.27[B]	91.3[o]
$^2P_{3/2}-^2P_{3/2}$	264.78	264.79[f]	232.50	232.49[n]	206.24	206.24[m]	184.36	184.34[o]	165.75	165.64[o]		114.08[o]
$^2P_{3/2}-^2P_{1/2}$	270.48	270.52[f]	237.85	237.87[n]	210.88	211.03[m]	188.47[B]	188.37[o]	168.98[B]	169.06[o]	112.23[B]	112.16[o]
$^2P_{1/2}-^2S_{1/2}$		274.20[f]	239.50	239.53[n]	211.67	211.60[m]	188.47[B]	188.42[o]	168.98[B]	168.87[o]	112.23[B]	112.17[o]
$^2P_{1/2}-^2D_{3/2}$	334.22	334.17[f]	288.18	288.17[p]		249.34[m]	220.96	220.88[o]	194.54	194.44[o]	122.37	122.40[o]
$^2P_{3/2}-^2D_{5/2}$		353.83[f]	309.11	309.18[p]		272.09[m]	242.76	242.8[o]	216.91	216.86[o]	140.78	140.77[o]

Si I

	Fe XIII		Ni XV		Zn XVII		Ge XIX		Se XXI		Mo XXIX	
$3s^23p^2$-$3s3p^3$												
$^3P_0$-$^3S_1$	240.71	240.71[f]	209.25	209.18[n]	183.47	183.51[m]						
$^3P_1$-$^3S_1$		246.21[f]	215.90[B]	215.94[n]	191.54	191.57[m]						
$^3P_2$-$^3S_1$	251.98	251.95[f]	221.93	221.93[n]	197.45	197.58[m]						
$^1D_2$-$^1P_1$	256.42	256.42[q]		224.04[n]								
$3s^23p^2$-$3s^23p3d$												
$^1D_2$-$^1F_3$	196.56	196.53[f]	173.67	173.73[n]	155.70	155.75[m]	141.20		129.06[B]		96.04	
$^3P_1$-$^3D_2$	200.09	200.02[f]		174.99[n]		155.04[m]						
$^3P_1$-$^3D_1$	201.17	201.12[f]	176.10	176.10[n]		162.21[m]						
$^3P_0$-$^3P_1$	202.02	202.04[f]	176.64	176.69[f]		150.85[m]						
$^3P_2$-$^3D_2$	203.82[B]	203.79[f]	178.81	178.87[n]		158.98[m]						
$^3P_2$-$^3D_3$	203.82[B]	203.83[f]	179.23	179.27[f]	159.43	159.47[m]	142.93	143.04[k]	129.06[B]	129.5[s]	88.12	88.3[y]
$^3P_2$-$^3D_1$	204.97	204.94[f]		180.06[n]								
$^1S_0$-$^1P_1$	208.67	208.68[f]		184.06		165.03[m]						
$^3P_2$-$^3P_2$	213.76	213.77[f]	189.20	189.21[n]		169.69[m]						
$^1D_2$-$^1D_2$	221.81	221.82[f]	195.51	195.52[n]								

P I

	Fe XII		Ni XIV		Zn XVI		Ge XVIII		Se XX		Mo XXVIII
$3s^23p^3$-$3s^23p^2(^3P)3d$											
$^2D_{3/2}$-$^2F_{5/2}$	186.84[8]	186.86[q]									
$^2D_{5/2}$-$^2F_{7/2}$	186.84[8]	186.88[f]	164.12	164.13[f]	146.17	146.23[m]	131.46	131.3[s]	119.05	119.7[s]	
$^2P_{3/2}$-$^2D_{5/2}$	191.08	191.05[f]	168.33	168.37[n]							
$^4S_{3/2}$-$^4P_{3/2}$	193.48	193.51[f]		169.68[f]							
$^4S_{3/2}$-$^4P_{5/2}$	195.14	195.12[f]	171.38	171.36[f]	152.38	152.40[m]	136.70	136.7[s]	123.38	123.3[s]	
$3s^23p^3$-$3s^23p^2(^1D)3d$											
$^2P_{1/2}$-$^2P_{3/2}$	198.60	198.56[f]		173.74[n]							

S I

	Fe XI		Ni XIII		Zn XV		Ge XVII		Se XIX		Mo XXVII
$3p^4$-$3p^3(^4S)3d$											
$^3P_2$-$^3D_2$		178.06[f]	155.09	155.12[n]	137.13	137.06[m]					
$^3P_2$-$^3D_3$	180.35[B]	180.40[f]	157.65[B]	157.73[r]		139.85[m]	125.04	125.0[s]	112.38	112.5[s]	
$^3P_0$-$^3D_1$	181.10	181.13[f]		158.77[n]							
$^3P_1$-$^3D_2$	182.16	182.17[f]	159.97[B]	159.97[n]		142.74[m]					
$3p^4$-$3p^3(^2D)3d$											
$^1D_2$-$^1F_3$	179.80	179.76[f]	157.65[B]	157.55[n]		140.43[m]	126.52	126.4[s]	113.94	114.0[s]	
$^1D_2$-$^1D_2$		184.79[f]	161.57	161.56[n]	143.74	143.68[m]					
$^3P_1$-$^3P_1$	189.12	189.12[f]									
$^3P_1$-$^3P_2$	192.80	192.81[f]		169.59[n]							
$3p^4$-$3p^3(^2P)3d$											
$^3P_2$-$^3P_2$	201.63	201.58[r]			151.72	151.77[m]					

Cl I

	Fe X		Ni XII		Zn XIV		Ge XVI		Se XVIII		Mo XXVI	
$3p^5$-$3p^4(^3P)3d$												
$^2P_{3/2}$-$^2D_{5/2}$	174.53	174.53[f]	152.12	152.15[r]	134.71	134.80[m]	120.81	120.9[s]	109.19	109.1[s]	76.73	76.6y
$^2P_{1/2}$-$^2D_{3/2}$	175.28	175.26[f]	152.88	152.95[n]	135.60	135.59[m]		121.8[s]		109.9[s]		80.0y
$^2P_{3/2}$-$^2P_{3/2}$	177.21	177.24[f]	154.15	154.18[r]	136.30	136.31[m]	121.79		109.97[B]			75.2y
$3p^5$-$3p^4(^1D)3d$												
$^2P_{3/2}$-$^2S_{1/2}$	184.50	184.54[f]	160.53	160.56[n]	138.28[B]	138.18[m]						78.4y
$^2P_{1/2}$-$^2S_{1/2}$	190.03	190.04[f]		166.88[n]		145.03[m]						
$^2P_{3/2}$-$^2D_{3/2}$	230.10	230.13[r]										
$^2P_{3/2}$-$^2P_{1/2}$					174.75	174.70[m]						72.7y
$3p^5$-$3p^4(^1S)3d$												
$^2P_{1/2}$-$^2D_{3/2}$					153.71	153.69[m]						
$^2P_{3/2}$-$^2D_{3/2}$												79.3y

Ar I

	Fe IX		Ni XI		Zn XIII		Ge XV		Se XVII		Mo XXV	
$3p^6$-$3p^5 3d$												
$^1S_0$-$^1P_1$	171.07	171.07[f]	148.35	148.37[r]	130.99	131.06[m]	117.23	117.25[k]	105.85	105.9[s]	74.26	74.1[y]
$^1S_0$-$^3D_1$		217.10[f]	186.99	186.98[w]	164.06[B]		145.77		131.06		91.27[B]	
$^1S_0$-$^3P_1$	244.84	244.91[f]	211.44	211.44[w]	186.13		166.41		150.32[B]		108.25	

K I

	Fe VIII		Ni X		Zn XII		Ge XIV		Se XVI		Mo XXIV	
$3p^6 3d$-$3p^5 3d^2(^3F)$												
$^2D_{3/2}$-$^2D_{3/2}$	167.53	167.49[f]	144.26	144.21[r]	126.74	126.74[m]	112.94	112.96[k]	101.69	102.2[s]	70.80	70.7[y]
$^2D_{5/2}$-$^2D_{5/2}$	168.20	168.17[f]	144.98	144.99[r]	127.63	127.62[m]	113.81	113.93[k]	102.69	102.6[s]	72.12	72.1[y]
$^2D_{5/2}$-$^2F_{7/2}$	185.17	185.22[f]	158.34	158.37[#]	138.28[B]	138.42[m]	122.76[B]	122.82[k]	109.97[B]	109.9[s]		75.0[y]
$^2D_{3/2}$-$^2F_{5/2}$		186.61[f]	159.97[B]	159.98[#]	140.10	140.12[m]						78.9[y]
$3p^6 3d$-$3p^5 3d^2(^3P)$												
$^2D_{5/2}$-$^2P_{3/2}$	168.53	168.55[f]	145.80	145.78[#]		128.01[m]					71.24	71.2[y]

[a]B. Edlen, Ref. 27

[b]B. Edlen, Ref. 28

[c]B. Edlen, Ref. 30

[d]Behring et al., Ref. 20

[e]B. Edlen, Ref. 29

[f]Behring et al., Ref. 11

[g]Reader et al., Ref.25

[h]Kononov et al., Ref. 14

[i]Lawson and Peacock, Ref. 21

[j]Burkhalter et al., Ref. 12

[k]Fawcett and Hayes, Ref. 10

[l]Reader, Ref. 18

[m]Sugar and Kaufman, Ref. 23

[n]Fawcett and Hayes, Ref. 7

[o]Hinnov et al., Ref. 22

[p]Fawcett and Hatter, Ref. 15

[q]Bromage et al., Ref. 13

[r]Behring et al., Ref. 6

[s]Stratton et al., Ref. 17

[t]Feldman et al., Ref. 26

[u]Peacock et al., Ref. 19

[v]Fawcett et al., Ref. 8

[w]Svensson et al., Ref. 9

[x]Finkenthal et al., Ref. 16

[y]Finkenthal et al., Ref. 24

[z]Edlen, Ref. 31

[#]Goldsmith and Fraenkel, Ref. 5

[B]Blend.

[S]Observed in second order.

FIGURE CAPTIONS

Fig. 1 Spectra recorded at intervals of 50 ms during a PLT discharge. Spectrum (a) was recorded just before injection and spectra (b) and (c) were recorded after injection of Mo.

Fig. 2 Mo spectrum in the wavelength region 60-105 Å.

Fig. 3 Mo spectrum in the wavelength region 95-145 Å.

Fig. 4 Mo spectrum in the wavelength region 155-215 Å.

Fig. 5 Mo spectrum in the wavelength region 220-295 Å.

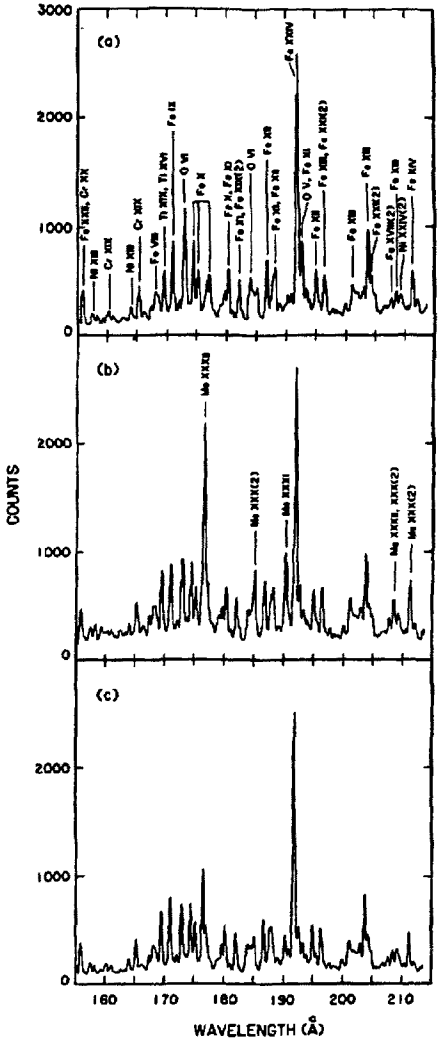
(a)
(b)
(c)
COUNTS
WAVELENGTH (Å)
3000
2000
1000
0
160
170
180
190
200
210

FIGURE 1

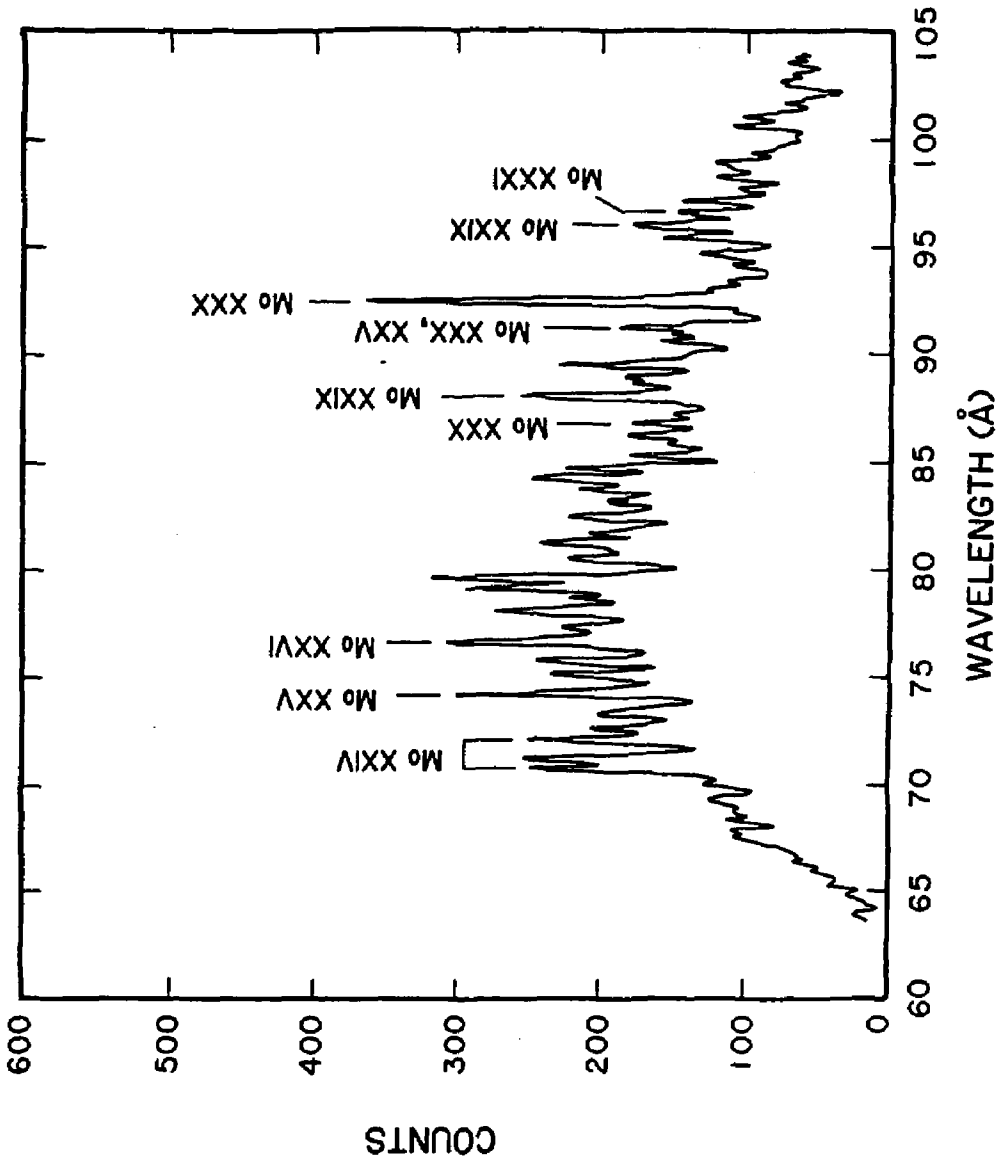
Mo XXXI
Mo XXIX
Mo XXX
Mo XXX, XXV
Mo XXIX
Mo XXX
Mo XXVI
Mo XXV
Mo XXIV
COUNTS
0
100
200
300
400
500
600
WAVELENGTH (Å)
60
65
70
75
80
85
90
95
100
105

FIGURE 2

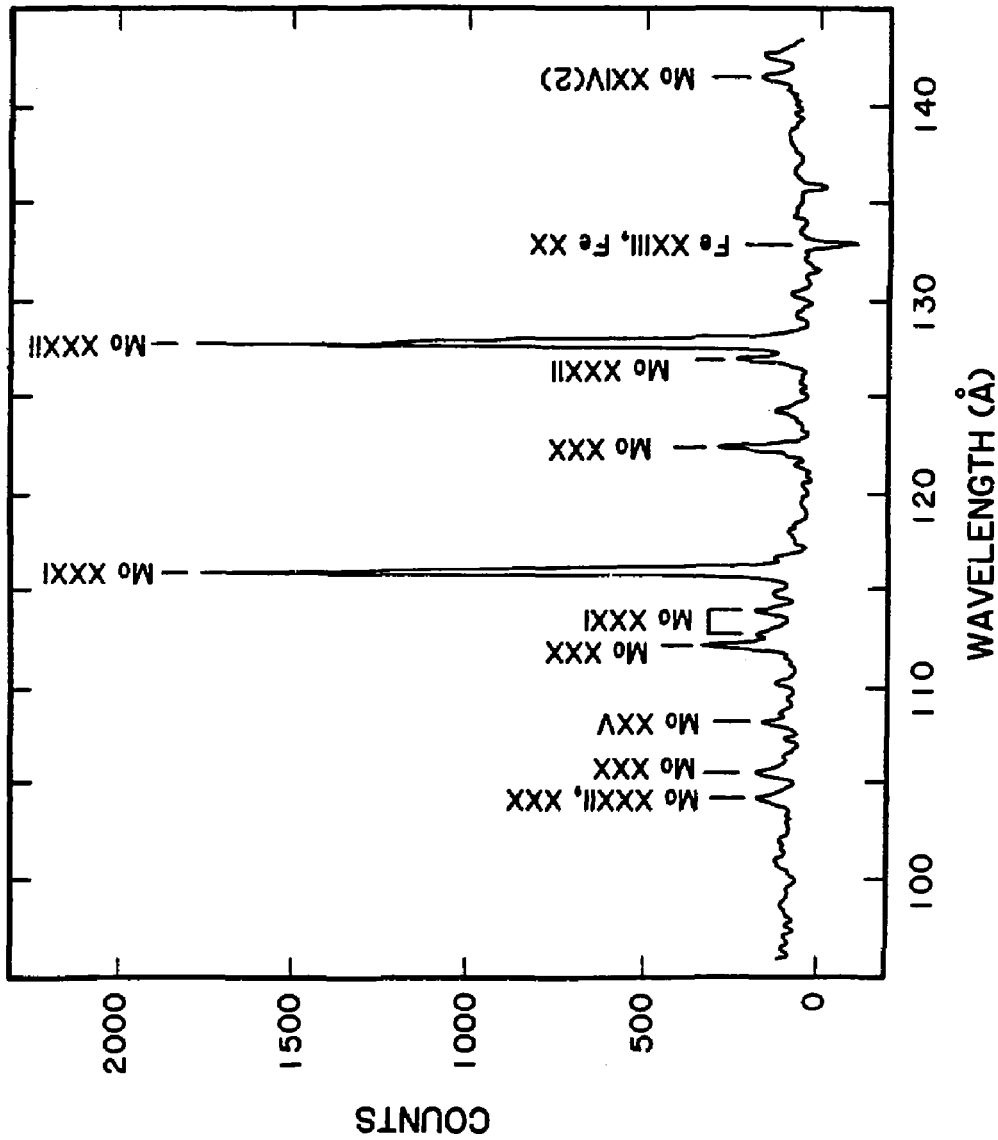
Mo XXIV(2)
Fe XXIII, Fe XX
Mo XXXII
Mo XXXII
Mo XXX
Mo XXXI
Mo XXXI
Mo XXX
Mo XXV
Mo XXX
Mo XXXII, XXX
2000
1500
1000
500
0
COUNTS
100
110
120
130
140
WAVELENGTH (Å)

FIGURE 3

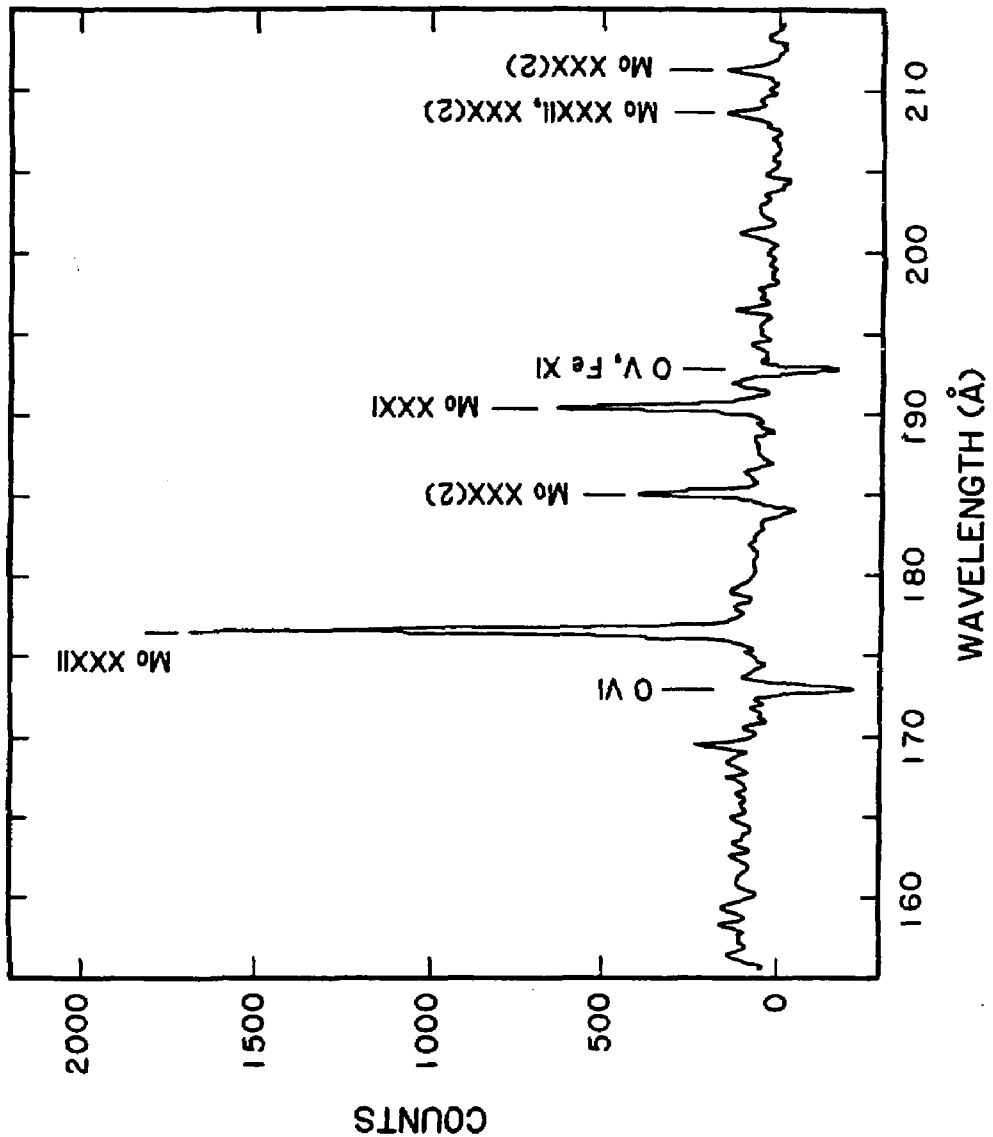
COUNTS
2000
1500
1000
500
0
160
170
180
190
200
210
WAVELENGTH (Å)
Mo XXXII
O VI
Mo XXX(2)
Mo XXXI
O V, Fe XI
Mo XXXII, XXX(2)
Mo XXX(2)

FIGURE 4

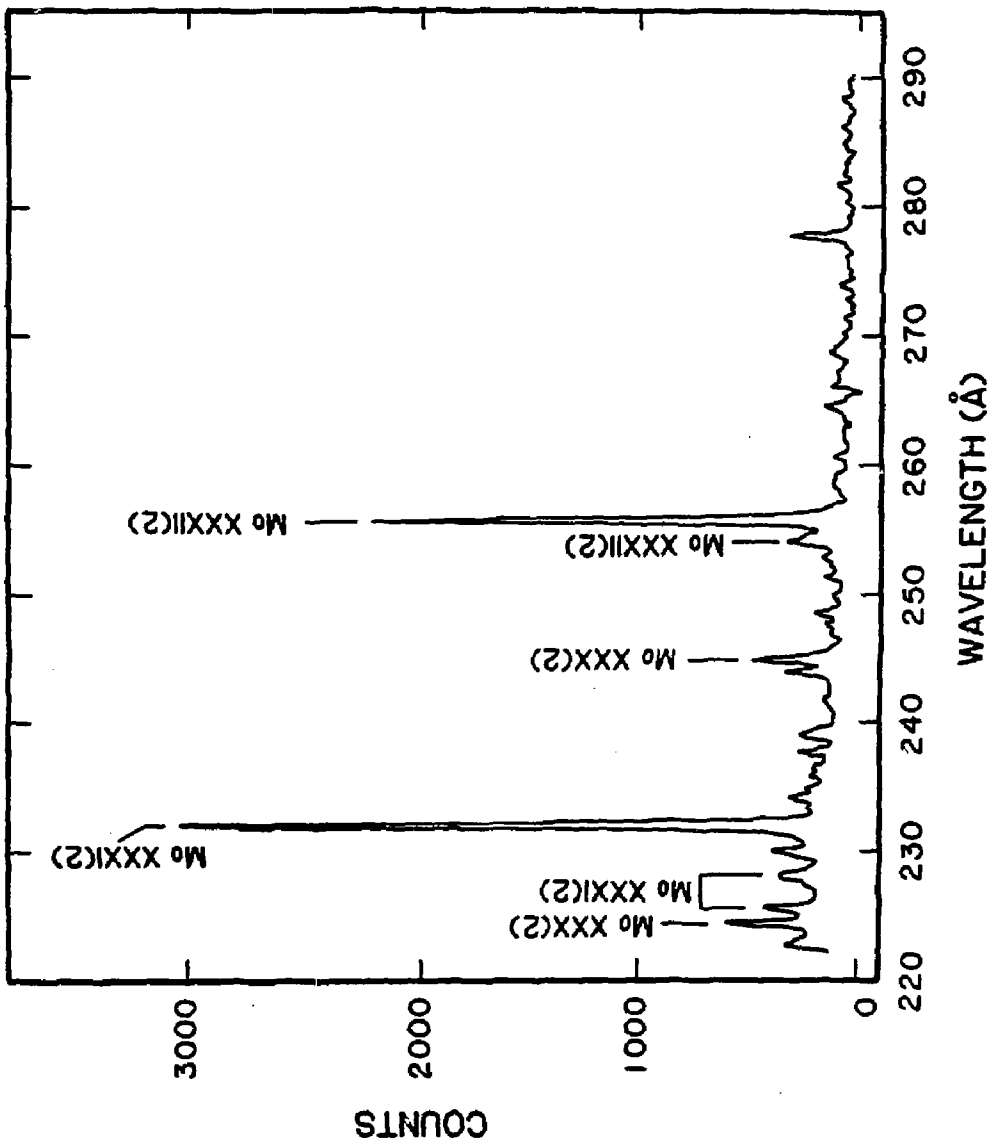
COUNTS
3000
2000
1000
0
220
230
240
250
260
270
280
290
WAVELENGTH (Å)
Mo XXXI(2)
Mo XXX(2)
Mo XXXI(2)
Mo XXX(2)
Mo XXXII(2)
Mo XXXII(2)

FIGURE 5

EXTERNAL DISTRIBUTION IN ADDITION TO UC-20

Dr. Frank J. Paoloni, Univ of Wollongong, AUSTRALIA
Prof. M.H. Brennan, Univ Sydney, AUSTRALIA
Plasma Research Lab., Australian Nat. Univ., AUSTRALIA
Prof. I.R. Jones, Flinders Univ., AUSTRALIA
Prof. F. Cap, Inst Theo Phys, AUSTRIA
Prof. M. Heindler, Institut fur Theoretische Physik, AUSTRIA
M. Goossens, Astronomisch Instituut, BELGIUM
Ecole Royale Militaire, Lab de Phys Plasmas, BELGIUM
Commission-European, Dg-XII Fusion Prog, BELGIUM
Prof. R. Boucique, Laboratorium voor Natuurkunde, BELGIUM
Dr. P.H. Sakanaka, Instituto Fisica, BRAZIL
Instituto De Pesquisas Espaciasi-INPE, BRAZIL
Documents Office, Atomic Energy of Canada Limited, CANADA
Dr. M.P. Bachynski, MPB Technologies, Inc., CANADA
Dr. H.M. Skarsgard, University of Saskatchewan, CANADA
Dr. H. Bernard, University of British Columbia, CANADA
Prof. J. Teichmann, Univ. of Montreal, CANADA
Prof. S.R. Sreenivasan, University of Calgary, CANADA
Prof. Tudor W. Johnston, INRS-Energie, CANADA
Dr. C.R. James, Univ. of Alberta, CANADA
Dr. Peter Lukac, Komenskeho Univ, CZECHOSLOVAKIA
The Librarian, Culham Laboratory, ENGLAND
The Librarian, Rutherford Appleton Laboratory, ENGLAND
Mrs. S.A. Hutchinson, JET Library, ENGLAND
C. Mouttet, Lab. de Physique des Milieux Ionises, FRANCE
J. Radet, CEN/CADARACHE - Bat 506, FRANCE
Univ. of Ioannina, Library of Physics Dept. GREECE
Dr. Tom Mual, Academy Bibliographic Ser., HONG KONG
Preprint Library, Hungarian Academy of Sciences, HUNGARY
Dr. S. Dasgupta, Saha Inst of Nucl. Phys., INDIA
Dr. P. Kaw, Institute for Plasma Research, INDIA
Dr. Phillip Rosenau, Israel Inst. Tech, ISRAEL
Librarian, Int'l Ctr Theo Phys, ITALY
Prof. G. Rostagni, Univ Di Padova, ITALY
Miss Clelia De Palo, Assoc EURATOM-ENEA, ITALY
Biblioteca, Instituto di Fisica del Plasma, ITALY
Dr. H. Yamato, Toshiba Res & Dev, JAPAN
Prof. I. Kawakami, Atomic Energy Res. Institute, JAPAN
Prof. Kyoji Nishikawa, Univ of Hiroshima, JAPAN
Direc. Dept. Large Tokamak Res. JAERI, JAPAN
Prof. Satoshi Itoh, Kyushu University, JAPAN
Research Info Center, Nagoya University, JAPAN
Prof. S. Tanaka, Kyoto University, JAPAN
Library, Kyoto University, JAPAN
Prof. Nobuyuki Inoue, University of Tokyo, JAPAN
S. Mori, JAERI, JAPAN
Librarian, Korea Advanced Energy Res. Institute, KOREA
Prof. D.I. Choi, Adv. Inst Sci & Tech, KOREA
Prof. B.S. Liley, University of Waikato, NEW ZEALAND
Institute of Plasma Physics, PEOPLE'S REPUBLIC OF CHINA
Librarian, Institute of Phys., PEOPLE'S REPUBLIC OF CHINA
Library, Tsing Hua University, PEOPLE'S REPUBLIC OF CHINA
Z. Li, Southwest Inst. Physics, PEOPLE'S REPUBLIC OF CHINA
Prof. J.A.C. Cabral, Inst Superior Tecnico, PORTUGAL
Dr. Octavian Petrus, AL I CUZA University, ROMANIA
Dr. Johan de Villiers, Fusion Studies, AEC, SO AFRICA
Prof. M.A. Hellberg, University of Natal, SO AFRICA
C.I.E.M.A.T., Fusion Div. Library, SPAIN
Dr. Lennart Stenflo, University of UMEA, SWEDEN
Library, Royal Inst Tech, SWEDEN
Prof. Hans Wilhelmson, Chalmers Univ Tech, SWEDEN
Centre Phys des Plasmas, Ecole Polytech Fed, SWITZERLAND
Bibliotheek, Fom-Inst Voor Plasma-Fysica, THE NETHERLANDS
Dr. D.D. Ryutov, Siberian Acad Sci, USSR
Dr. G.A. Eliseev, Kurchatov Institute, USSR
Dr. V.A. Glukhikh, Inst Electrophysical Apparatus, USSR
Dr. V.T. Tolok, Inst. Phys. Tech. USSR
Dr. L.M. Kovrizhnykh, Institute Gen. Physics, USSR
Nuclear Res. Establishment, Julich Ltd., W. GERMANY
Bibliothek, Inst. Fur Plasmaforschung, W. GERMANY
Dr. K. Schindler, Ruhr Universitat Bochum, W. GERMANY
ASDEX Reading Rm, IPP/Max-Planck-Institut fur Plasmaphysik, W. GERMANY
Librarian, Max-Planck Institut, W. GERMANY
Prof. R.K. Janev, Inst Phys, YUGOSLAVIA